Acta Cryst. (1973). A**29**, 453

The Information on Ordered Magnetic Structures which can be gained from Unpolarized-Neutron-Diffraction Data

BY C. WILKINSON AND E. J. LISHER*

Queen Elizabeth College, University of London, Campden Hill Road, London, W8 7AH, England

(*Received* 18 *December* 1972; *accepted* 11 *February* 1973)

The parameters which can be obtained from an unpolarized-neutron-diffraction investigation of an ordered magnetic structure are discussed in terms of the spin-density Patterson function. The effect of magnetic domains on the information available from a single-crystal experiment is considered and the treatment is extended to cover powder diffraction data. The symmetry of the spin-density Patterson function before and after domain averaging is described.

1. Introduction

It has been shown (Wilkinson, 1968, 1973) that a spin-density Patterson function may be computed from unpolarized-neutron diffraction data from a magnetic single crystal. The function has been used by Yessik (1968) in the establishment of the magnetic structure of Mn_2P and by Forsyth, Johnson & Wilkinson (1970) to assist in the solution of the magnetic structure of vivianite $Fe_3(PO_4)_2.8H_2O$.

The purpose of the present paper is to discuss in terms of this function the information which is available from single-crystal or powder unpolarized-neutron diffraction experiments. The problem has been partially tackled by Shirane (1959), who considered the information which could be obtained from powder diffraction data when the magnetic structure had a single spin axis. The present treatment is more general and applies to any magnetic structure and various diffraction situations. These will be considered individually.

2. Single-crystal data

2.1 *Single-domain single crystal*

As indicated in an earlier paper (Wilkinson, 1968) the magnetic intensity data from a single magnetic domain and a knowledge of the 'chemical' structure of a material in principle allow a direct determination of the magnetic structure. The information contained in the Patterson function can be extracted from the height and elongation of the Patterson peaks. This is developed more fully below.

Suppose there are N atoms in the magnetic unit cell with spins $\mathbf{S}^1$ to $\mathbf{S}^N$. The N^2 Patterson peak heights may be arranged in the symmetric matrix $\mathbf{Q}$ in which each element q_{mn} is the scalar product $\mathbf{S}^m \cdot \mathbf{S}^n$

Thus

$$\mathbf{Q}=\begin{pmatrix} \mathbf{S}^1\cdot\mathbf{S}^1 & \mathbf{S}^1\cdot\mathbf{S}^2 & \dots & \mathbf{S}^1\cdot\mathbf{S}^N \\ \mathbf{S}^2\cdot\mathbf{S}^1 & \mathbf{S}^2\cdot\mathbf{S}^2 & & \\ \vdots & & \ddots & \vdots \\ \mathbf{S}^N\cdot\mathbf{S}^1 & \dots\dots & & \mathbf{S}^N\cdot\mathbf{S}^N \end{pmatrix}.$$

(The peaks with heights q_{nn} are overlapped at the origin of the Patterson function where the peak height is $|\mathbf{S}^1|^2+|\mathbf{S}^2|^2+\dots|\mathbf{S}^N|^2$.).

The elongation of the peaks may be described by a 'vector' array $\mathbf{E}$ in which the element $\hat{\mathbf{e}}_{mn}$ is a unit vector in the direction of the elongation of the peak of height q_{mn}. This unit vector is the bisector of the spin directions $\mathbf{S}^m$, and $\mathbf{S}^n$.

Thus

$$\mathbf{E}=\begin{pmatrix} \hat{\mathbf{e}}_{11} & \hat{\mathbf{e}}_{12} & \dots & \hat{\mathbf{e}}_{1N} \\ \hat{\mathbf{e}}_{21} & \hat{\mathbf{e}}_{22} & & \\ \vdots & & \ddots & \vdots \\ \hat{\mathbf{e}}_{N1} & \dots\dots & & \mathbf{e}_{NN} \end{pmatrix}.$$

The elements of $\mathbf{E}$ may be used to determine the unit vectors $\hat{\mathbf{S}}^N$. Consider any three spins $\mathbf{S}^i$, $\mathbf{S}^j$, $\mathbf{S}^k$ for which the elements $\hat{\mathbf{e}}_{ij}$, $\hat{\mathbf{e}}_{ik}$, $\hat{\mathbf{e}}_{jk}$ are known.

Then

$$\hat{\mathbf{e}}_{ij}=\frac{\hat{\mathbf{S}}^i+\hat{\mathbf{S}}^j}{|\hat{\mathbf{S}}^i+\hat{\mathbf{S}}^j|},\quad \hat{\mathbf{e}}_{ik}=\frac{\hat{\mathbf{S}}^i+\hat{\mathbf{S}}^k}{|\hat{\mathbf{S}}^i+\hat{\mathbf{S}}^k|} \text{ and } \hat{\mathbf{e}}_{jk}=\frac{\hat{\mathbf{S}}^j+\hat{\mathbf{S}}^k}{|\hat{\mathbf{S}}^j+\hat{\mathbf{S}}^k|}.$$

These equations may be solved for $\hat{\mathbf{S}}^i$, $\hat{\mathbf{S}}^j$ and $\hat{\mathbf{S}}^k$, *e.g.*

$$\hat{\mathbf{S}}^i=\frac{(\hat{\mathbf{e}}_{jk}\cdot\hat{\mathbf{e}}_{ij})\hat{\mathbf{e}}_{ik}+(\hat{\mathbf{e}}_{ik}\cdot\hat{\mathbf{e}}_{jk})\hat{\mathbf{e}}_{ij}-(\hat{\mathbf{e}}_{ik}\cdot\hat{\mathbf{e}}_{ij})\hat{\mathbf{e}}_{jk}}{\sqrt{(\hat{\mathbf{e}}_{ij}\cdot\hat{\mathbf{e}}_{jk})^2+(\hat{\mathbf{e}}_{ik}\cdot\hat{\mathbf{e}}_{jk})^2+(\hat{\mathbf{e}}_{ij}\cdot\hat{\mathbf{e}}_{ik})^2-2(\hat{\mathbf{e}}_{ij}\cdot\hat{\mathbf{e}}_{jk})(\hat{\mathbf{e}}_{ik}\cdot\hat{\mathbf{e}}_{jk})(\hat{\mathbf{e}}_{ij}\cdot\hat{\mathbf{e}}_{ik})}}.$$

Knowing $\hat{\mathbf{S}}^i$, $\hat{\mathbf{S}}^j$ and $\hat{\mathbf{S}}^k$ and the elements q_{ij}, q_{jk}, q_{ik} the values of $|\mathbf{S}^i|$, $|\mathbf{S}^j|$ and $|\mathbf{S}^k|$ can be determined from expressions of the type

* Now at the Department of Physics, University of St. Andrews, Fife, Scotland.

$$|\mathbf{S}^i| = \sqrt{\frac{q_{ij}q_{ik}(\hat{\mathbf{S}}_j \cdot \mathbf{S}_k)}{q_{jk}(\hat{\mathbf{S}}_i \cdot \hat{\mathbf{S}}_j)\,(\hat{\mathbf{S}}_j \cdot \hat{\mathbf{S}}_k)}}.$$

The above expressions show that in principle it is possible to solve the magnetic structure from the Patterson function for a single-domain single crystal. This is probably of academic interest, however, as single-domain single-crystal experiments are rare, and in many cases the elongations $\hat{\mathbf{e}}_{ij}$ are difficult to determine because of partial overlap of the Patterson peaks.

2.2 *Multi-domain single crystal*

When several equally populated magnetic domains occur within a single crystal the information available from an unpolarized-neutron diffraction experiment may be reduced. The effects of having several domains may be analysed in terms of the superposition of intensities in reciprocal space, or the superposition in real space of the Patterson peaks from each domain. The Patterson representation of the problem will be considered here.

The expression for a Patterson peak is computed from three-dimensional data is of the form

$$Q'(\mathbf{u}^{mn}+\mathbf{x}) = f_1(|\mathbf{x}|)\mathbf{S}^m \cdot \mathbf{S}^n + f_2(|\mathbf{x}|)\,(\mathbf{S}^m \cdot \hat{\mathbf{x}})\,(\mathbf{S}^n \cdot \hat{\mathbf{x}})$$

(Wilkinson, 1973),

where $f_1(|\mathbf{x}|)$ and $f_2(|\mathbf{x}|)$ are functions of the distance $|\mathbf{x}|$ from the centre of the peak at vector distance $\mathbf{u}^{mn}$ from the origin. The term involving $f_1(|\mathbf{x}|)$ is spherically symmetric and governs the peak height [$f_2(0)=0$], while the second term determines the peak elongation. The spins in a second magnetic domain (related to those of the first domain by the symmetry operators of the chemical space group of the material) will produce different magnetic intensities and consequently a different Patterson function. The peak positions in the second distribution will, however, be identical with those of the first and peak overlap will therefore occur when the distributions are superposed. The term $f_1(|\mathbf{x}|)\mathbf{S}^m \cdot \mathbf{S}^n$ is the same for both domains, but the peak elongations will be in different directions. This shows that although the size of the moments $\mathbf{S}^m$ and $\mathbf{S}^n$ and the angle between them may still be determined, some or all of the information may be lost concerning the angles between $\mathbf{S}^m$, $\mathbf{S}^n$ and crystallographic directions.

The above discussion of overlap can be put on a quantitative basis for the domains which occur in different crystal systems. This is set out in Appendix 1.

Although information may be lost from a particular peak as a result of overlap it is not necessarily lost from all peaks. Consider, for example, a hypothetical structure which has a chemical space group $P4$ and has magnetic atoms in the general equivalent positions x,y,z; $-y,x,z$; $y,-x,z$; $-x,-y,z$. Suppose that there are three magnetic structures for this material which exist at (say) different temperatures and these are shown in Fig. 1(*a*). *A* and *B* have magnetic structures which are commensurate with the chemical cell, while structure *C* has one edge of the original cell doubled. The spin directions have been chosen to lie parallel to the cell edges in the plane of the diagram. The magnetic space groups of *A*, *B* and *C* are monoclinic $P2$, tetragonal $P4$ and monoclinic $P_{2a}2$ respectively, and their 'configurational' groups are tetragonal $P4$,(*A*), triclinic $P1$,(*B*) and monoclinic $P2$,(*C*). Their configurational symmetries are shown in Fig. 1(*b*). [The notation used to represent magnetic space groups is that given by Opechowski & Guccione (1965).] The 'configurational' group is derived from the magnetic space group by assigning to each magnetic atom a scalar quantity which is identical for two atoms only if they have spins of the same magnitude and direction. It is therefore an ordinary 'chemical' space group, but is not in general identical with the 'chemical' space group of the material. It may belong to the same or a lower-symmetry crystal system.

The Patterson distributions for the domains shown in Fig. 1(*a*) are illustrated in Fig. 1(*c*). Elongated peaks are represented schematically by ellipses. Note that the origin peak for *B* is circular owing to the overlap of ellipses with major axes perpendicular. The height of the 'origin' peak is four times that of the subsidiary peaks in each case.

Since the material has chemical space group $P4$ there will be a total of four magnetic domains which are energetically equivalent and should therefore exist in equal volumes in the crystal. These will all contribute to the diffracted intensities and the nett effect on the Patterson distribution will be to superpose four distributions of the type in Fig. 1(*c*) each of which is relatively rotated by 90°. The result of this averaging procedure is shown in Fig. 1(*d*). It can be seen that there are no elongations in the distribution for model *A* and therefore nothing is known about the angle between the spin direction and the x, y axes, while in *B* the elongation of the negative elliptical peaks gives the spin direction and in *C* it is the lobes of the 'butterfly' which give the spin direction. (If the spins had been inclined to the basal plane then all peaks would also be elongated in the z-axis direction. This information remains after overlap and therefore any inclination to the basal plane is in principle detectable.) Consideration shows that it is the configurational symmetry of the magnetic structure which controls the information lost, as it is configurational symmetry which governs whether *all* of the overlapped peaks at any point are of the same type, while the domain types are governed by the symmetry of the chemical point group which is from a crystal system at least as high as that of the configurational group. In the example chosen information is lost concerning the absolute orientations of the spin directions and the x, y axes when the configurational symmetry is tetragonal.

A similar but more complex real example is found in the proposed models for the magnetic structure of $Mn_{1.9}Cr_{0.1}Sb$ from the single-crystal investigation by Austin, Adelson & Cloud (1963). These are shown in

Fig. 2 with their associated configurational symmetry and Patterson distributions. As stated by Austin *et al.* these two structures are indistinguishable by unpolarized-neutron diffraction, but it is interesting to note that this is true only after domain averaging. The two models do not therefore form a homometric Patterson pair in the true sense.

Using the results from Appendix 1 a table (Table 1) can be drawn up to indicate the parameters which may be determined from different configurational symmetries.

Table 1. *Parameters which may be determined from models with different configurational symmetries*

Configuration symmetry of model	Parameters which may be determined
Cubic	Magnitudes of spins and relative angles between spins
Tetragonal Hexagonal Trigonal	Magnitudes of spins and relative angles between them. Angles between spin directions and principal axis.
Orthorhombic Monoclinic Triclinic	All parameters

3. Powder diffraction data

The above discussion may with very little alteration be applied to powder diffraction data. In this case the 'domain' problem can still be relevant if the domain size is less than the crystallite size, and in any case, since the crystallites are assumed to adopt all possible orientations in the powder the 'domains' are effectively present even if each crystallite is a single domain. The superposed-Patterson-distribution approach can again be used and shows that when the model has cubic configurational symmetry it is possible only to determine the magnitudes and relative angles between the spin directions from a powder pattern. No information can be gained on the angle between any spin direction and a crystallographic direction. In the unaxial systems the additional information of the angles between spin directions and the principal axis may be evaluated, while in the orthorhombic, monoclinic and triclinic systems it is theoretically possible to determine all parameters from the powder pattern.

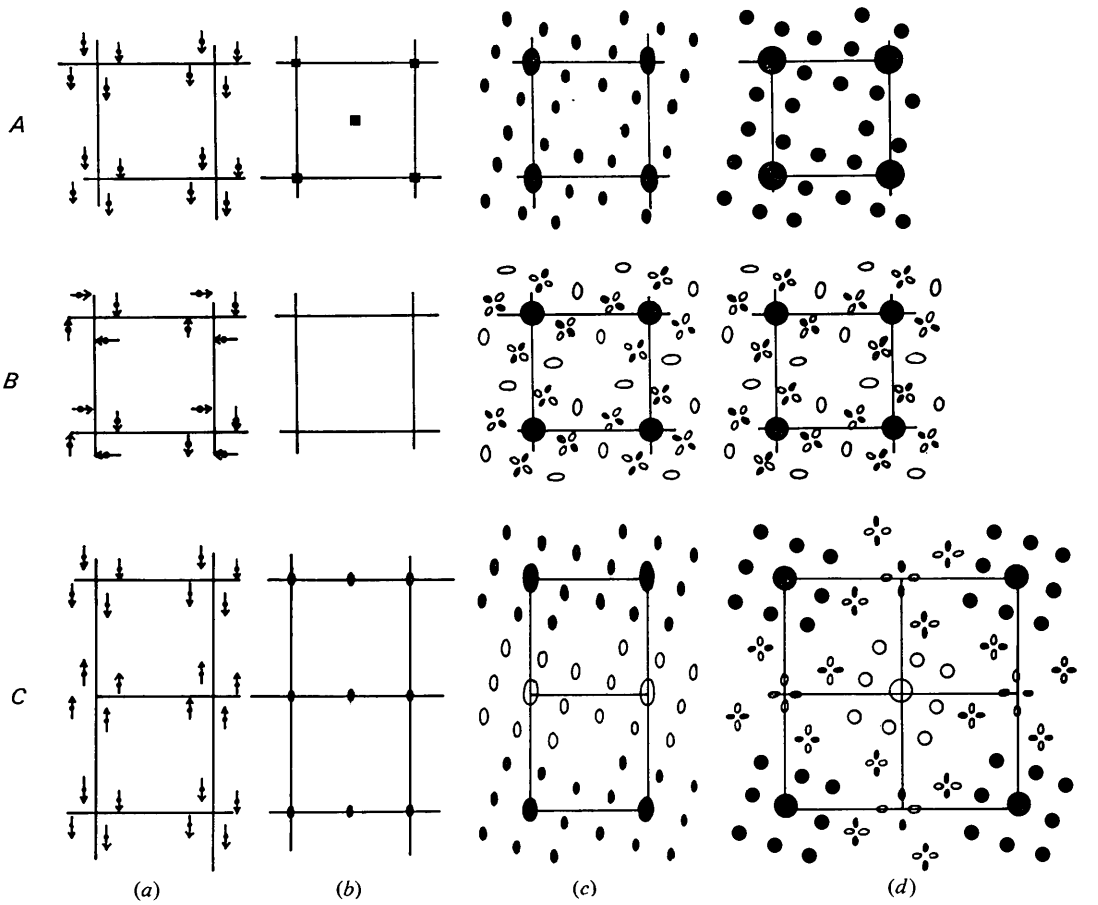

Fig. 1. (*a*) The spin arrangement, (*b*) configurational symmetry (*c*), single-domain Patterson function and (*d*) multidomain Patterson function for a hypothetical structure with chemical space group $P4$ and magnetic space groups $P2$ (*A*), $P4$(*B*) and $P_{2a}2$(*C*).

This agrees with the conclusion reached by Shirane (1959) who considered the special case of powder patterns of materials with a single spin axis. (His treatment concerned the averaging of overlapped intensities in reciprocal space.) It is interesting to consider the real space averaging of Patterson functions for the case of the MnO structure type, an example also considered by Shirane. The structure type proposed by Shull, Strauser & Wollan (1951) is shown in Fig. 3(*a*). Also shown is an alternative structure type suggested by Li (1955) which gives an intensity distribution independent of spin direction and the same as the Shull model with ⟨100⟩ spin direction. The configurational symmetry of the two models is shown in Fig. 3(*b*). The Shull model has trigonal configurational symmetry $R\bar{3}$ while the Li model has cubic configurational symmetry $F23$. No informa-

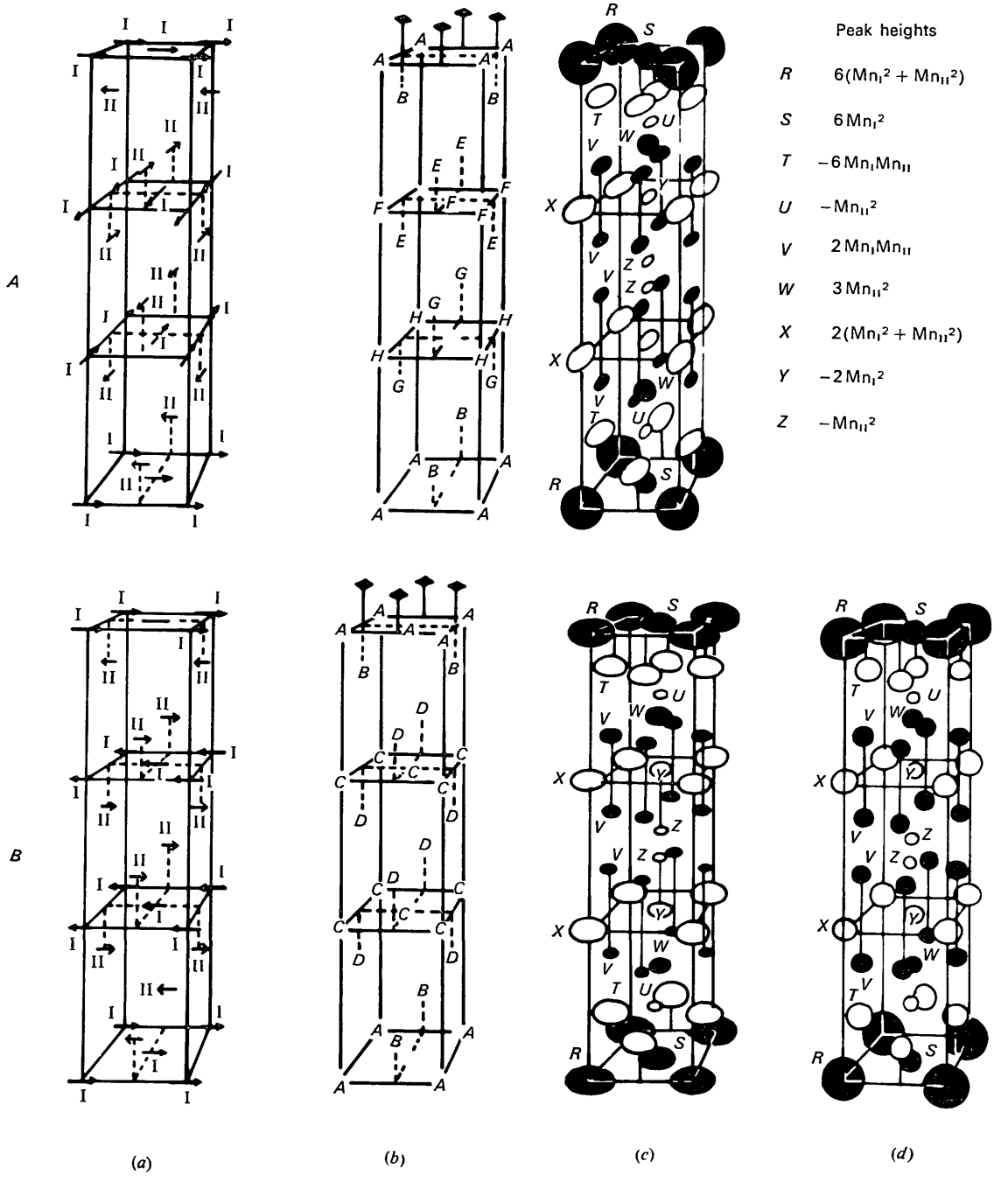

Fig. 2. (*a*) The spin arrangement, (*b*) configurational symmetry, (*c*) single-domain Patterson function and (*d*) multidomain Patterson function of alternative models for the magnetic structure of $Mn_{1.9}Cr_{0.1}Sb$. (*d*) is identical for structures *A* and *B*.

tion about the spin direction can therefore be obtained from the Li model, while on the Shull model the intensity distribution will be a function of the angle between the spin direction and the configurational triad.

The Patterson functions for single domains are given in Fig. 3(*c*). The ellipsoids have their major axes parallel to the spin direction. Averaging over the domains which have spin directions related by the indicated triad gives Patterson functions shown in Fig. 3(*d*). These are the '*S*'-type domains described by Roth (1960). The overlapped ellipsoid elongation (or contraction) is now parallel to this triad. For an original spin inclination of 54°44′ to the configurational triad the peaks are spherically symmetric. Averaging must also be performed over the '*T*' domain types, which have a different cubic triad as configurational axis. For the Li model this gives spherical peaks whatever the original spin direction, while for the Shull model the result is dependent on the original spin direction. Fig. 4 shows the Patterson peak distribution for the Shull model when the spin directions is (*a*) in a {111} plane, (*b*) at an angle of 54°44′ to ⟨111⟩, (*c*) in a ⟨111⟩ direction. (Fig. 4(*b*) corresponds to any spin direction in the case of the Li model.) The differences in the Patterson distributions are small and involve only changes of the 'butterfly' features as the angle between the spin direction and the triad alters. This explains why the different models give very similar powder diffraction intensities.

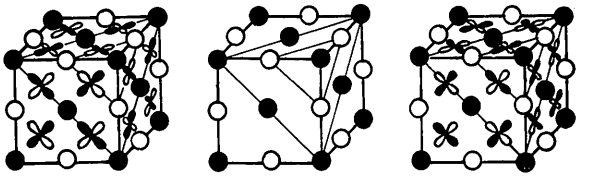

Fig. 4. Total domain-averaged Patterson distribution for the Shull model for MnO when the spin direction is (*a*) in a {111} plane (*b*) at an angle of 54°44′ to ⟨111⟩, (*c*) in a ⟨111⟩ direction.

4.1. Symmetry of the Patterson function for a single-domain single crystal

The space group of the Patterson distribution (vector set) calculated from unpolarized-neutron diffraction intensities from a single-domain single crystal is related to the magnetic space group (fundamental set) of the spin structure in a way very similar to that described by Buerger (1950) for the chemical space groups. As Buerger showed, there are 24 'chemical ' vector sets derived from the space groups of the 230 fundamental sets by substituting at the lattice points of vector space the translation-free residue of each generating element in the fundamental set, completing the group by forming the products of the operations of these elements with the lattice. A further requirement is that the vector space group should contain a centre of symmetry if one is not already present in the fundamental group.

This is still true of the 55 vector sets which can be derived from the 1421 magnetic space groups which may be used to represent ordered magnetic structures. There are, however, two additional requirements relating to operations involving time inversion. These are:

(i) A lattice translation of the fundamental set which involves time inversion becomes a black/white translation in the vector set. 22 of the 36 magnetic Bravais lattices contain time-inversion operators.

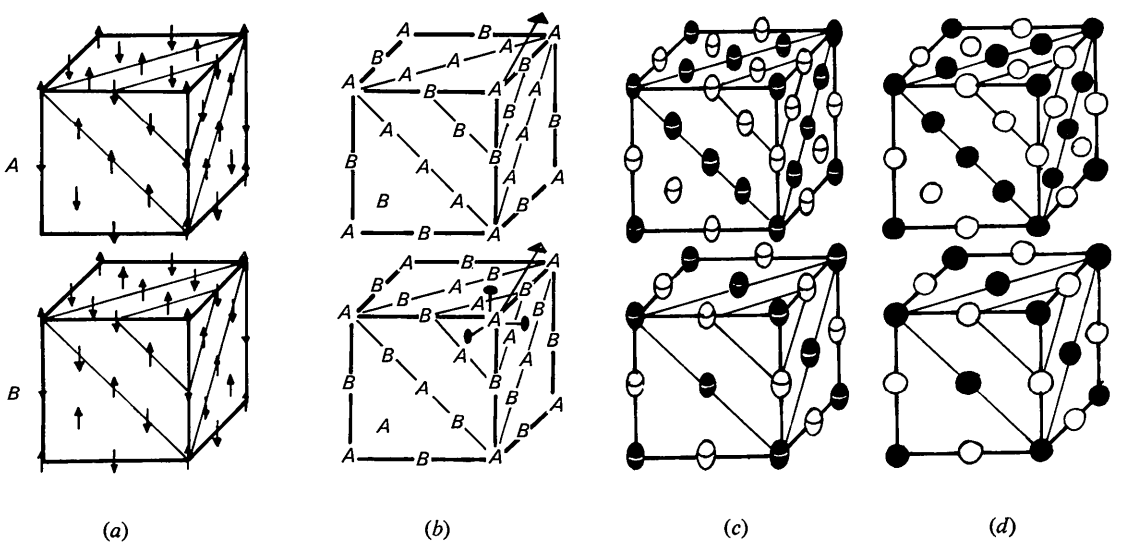

Fig. 3. The magnetic structure proposed by Shull (*A*) and by Li (*B*) for MnO. (*a*) illustrates the spin arrangement, (*b*) the configurational symmetry, (*c*) the single-domain Patterson function and (*d*) the Patterson distribution after averaging over '*S*' domains.

(ii) The symmetry elements at the lattice points of the vector set must not only be translation-free but time-inversion-free residues of the generating elements in the fundamental set,

i.e. $m'\ a'\ b'\ c'\ n'\ d'\ \bar{1}'\ 2'2_1'\ \bar{3}'\ 4'\bar{4}'4_1'4_2'4_3'\ 6'\bar{6}'6_1'6_2'6_3'6_4'6_5'$

becomes

$m\ a\ b\ c\ n\ d\ \bar{1}\quad 2\quad 3\quad\quad 4\quad\quad\quad 6.$

The extended form of the theorem of Buerger is therefore: 'If the fundamental set contains a given symmetry element, the vector set contains the parallel, translation-free and time-inversion-free residue of that symmetry element through the origin. Lattice translations involving time inversion in the fundamental set become black/white translations in the vector set. This will of course still apply to chemical space groups where time inversion is trivial.

A list of the space groups of the 55 Patterson vector sets which correspond to the fundamental sets of the 1421 magnetic space groups is given in Table 2. In Table 3 the magnetic space groups of the monoclinic system are listed with their corresponding vector-set space groups as an illustration of the way in which the vector-set groups are formed.

A diagrammatic example of the application of this theorem is given in Fig. 5, where the magnetic space group $Pn'm'a$ is illustrated with its effects on the three spin components of an atom in the general equivalent position 8(*d*). This is the magnetic space group of $HoFeO_3$ (Koehler, Wollan & Wilkinson, 1960) and is used by Atoji (1965) as an example of his graphical representation of magnetic space groups. The Atoji conventions have been adopted in depicting the symmetry operators in Fig. 5(*d*). The Patterson distribution is also illustrated in Fig. 5(*e*). The poles on the sterograms which have been drawn at positions corresponding to Patterson peaks for position 8(*d*) represent the elongation

Table 2. *The 55 vector sets derived from the* 1421 *magnetic space groups*

Triclinic	$P\bar{1}$, $P_{2_s}\bar{1}$.
Monoclinic	$P2/m$, $P_{2a}2/m$, $P_{2b}2/m$, P_C2/m, $C2/m$, $C_{2c}2/m$, C_P2/m.
Orthorhombic	$Pmmm$, $P_{2a}mmm$, P_Cmmm, P_Fmmm, $Cmmm$, $C_{2c}mmm$, C_Pmmm, C_Immm, $Fmmm$, F_Cmmm, $Immm$, I_Pmmm
Tetragonal	$P4/m$, $P_{2c}4/m$, $P_{a+b,a-b}4/m$, P_I4/m, $I4/m$, I_P4/m, $P4/mmm$, $P_{2c}4/mmm$, $P_{a+b,a-b}4/mmm$, P_I4/mmm, $I4/mmm$ I_P4/mmm.
Trigonal	$P\bar{3}$, $P_{2c}\bar{3}$, $R\bar{3}$, $R_R\bar{3}$, $P\bar{3}1m$, $P_{2c}\bar{3}1m$, $R\bar{3}m$, $R_R\bar{3}m$.
Hexagonal	$P6/m$, $P_{2c}6/m$, $P6/mmm$, $P_{2c}6/mmm$.
Cubic	$Pm3$, P_Fm3, $Fm3$, $Im3$, I_Pm3, $Pm3m$, P_Fm3m, $Fm3m$, $Im3m$, I_Pm3m.

Table 3. *Space groups of the fundamental sets for the monoclinic system and their corresponding vector sets*

Space group of fundamental set	Space group of vector set
$P2$, $P2'$, $P2_1$, $P2_1'$, Pm, Pm', Pc, Pc', $P2/m$, $P2'/m$, $P2/m'$, $P2'/m'$, $P2_1/m$, $P2_1'/m$, $P2_1/m'$, $P2_1'/m'$, $P2/c$, $P2'/c$, $P2/c'$, $P2'/c'$ $P2_1/c$, $P2_1'/c$, $P2_1/c'$, $P2_1'/c'$.	$P2/m$
$P_{2a}2$, $P_{2a}2_1$ $P_{2a}m$, $P_{2c}m'$, $P_{2a}c$, $P_{2a}2/m$, $P_{2c}2/m'$, $P_{2a}2_1/m$, $P_{2c}2_1/m'$, $P_{2a}2/c$, $P_{2a}2_1/c$	$P_{2a}2/m$
$P_{2b}2$, $P_{2b}2'$, $P_{2b}m$, $P_{2b}c$, $P_{2b}2/m$, $P_{2b}2/m$, $P_{2b}2/c$, $P_{2b}2'/c$,	$P_{2b}2/m$
P_C2 P_Cm, P_Cc P_C2/m, P_C2/c.	P_C2/m
$C2$, $C2'$ Cm, Cm', Cc, Cc'. $C2/m$, $C2'/m$, $C2/m'$, $C2'/m$,' $C2/c$, $C2'/c$, $C2/c'$, $C2'/c'$.	$C2/m$
$C_{2c}2$, $C_{2c}m$, $C_{2c}m'$, $C_{2c}2/m$, $C_{2c}2/m'$.	$C_{2c}2/m$
C_P2, C_P2', C_Pm, C_Pm', C_Pc, C_P2/m, C_P2'/m, C_P2/m', C_P2'/m', C_P2/c, C_P2'/c.	C_P2/m

directions of overlapped peaks. The symmetry of this distribution is *Pmmm* [Fig. 5(*f*)].

The black/white lattice tranlation is illustrated in Fig. 1 where the monoclinic magnetic space group $P_{2a}2$ has a Patterson function with space group $P_{2a}2/m$.

4.2. Symmetry of the Patterson distribution for a multi-domain single crystal

The spin directions of the magnetic domains which exist in a single crystal are related by the parent point group of the chemical space group. The Patterson distribution for the superposed domains may be generated by operating the point-group symmetry elements on the Patterson distribution for a single domain. This is illustrated by the structure *C* in Fig. 1 which has a single-domain monoclinic Patterson symmetry of $P_{2a}2/m$ and a chemical point group 4, producing a domain-averaged Patterson function with tetragonal space group $P_{a+b,a-b}4/m$. In the case of MnO the domain-averaged Patterson function has space group P_Fm3m and is generated by the chemical point group $m3m$ operating on the monoclinic single-domain Patterson function with space group $C_{2c}2/m$.

5. Discussion

The real value of the Patterson function must lie in the assistance which it gives in formulating a model from diffraction data for the magnetic structure of a particular material. The domain-averaging problem often reduces the information available, but in some cases the Patterson distributions from different domains may be identical when superposed. This is the case for vivianite [$Fe_3(PO4)_2.8H_2O$] which has been shown by Forsyth, Johnson & Wilkinson (1970) to have a monoclinic antiferromagnetic structure with spin directions in the plane perpendicular to the diad axis. The chemical point group is $2/m$ and the spin directions in the two domains are therefore at 180° to each other, making the superposition of the two Patterson distributions trivial.

In general, however, this will not be so and it may be difficult to disentangle the symmetry of an individual domain from the averaged distribution. There are, however, features which often appear in domain-averaged distributions (especially in antiferromagnets) which can give a clue that several domains are present. For example, in the case of structure C of Fig. 1(*c*) the single-domain Patterson $P_{2a}2/m$ produces the tetragonal group $P_{a+b,a-b}4/m$[Fig. 1(*d*)] when domain-averaged, but the 'butterfly' features which appear in Fig. 1(*d*) often indicate domain overlap. Here they are produced by the overlap of equal positive and negative elliptical peaks with their major axes perpendicular. They also occur in the domain-averaged MnO Patterson maps for similar reasons and are often found where domain averaging has taken place. Their appearance is not conclusive evidence of overlap as a similar feature is produced in a

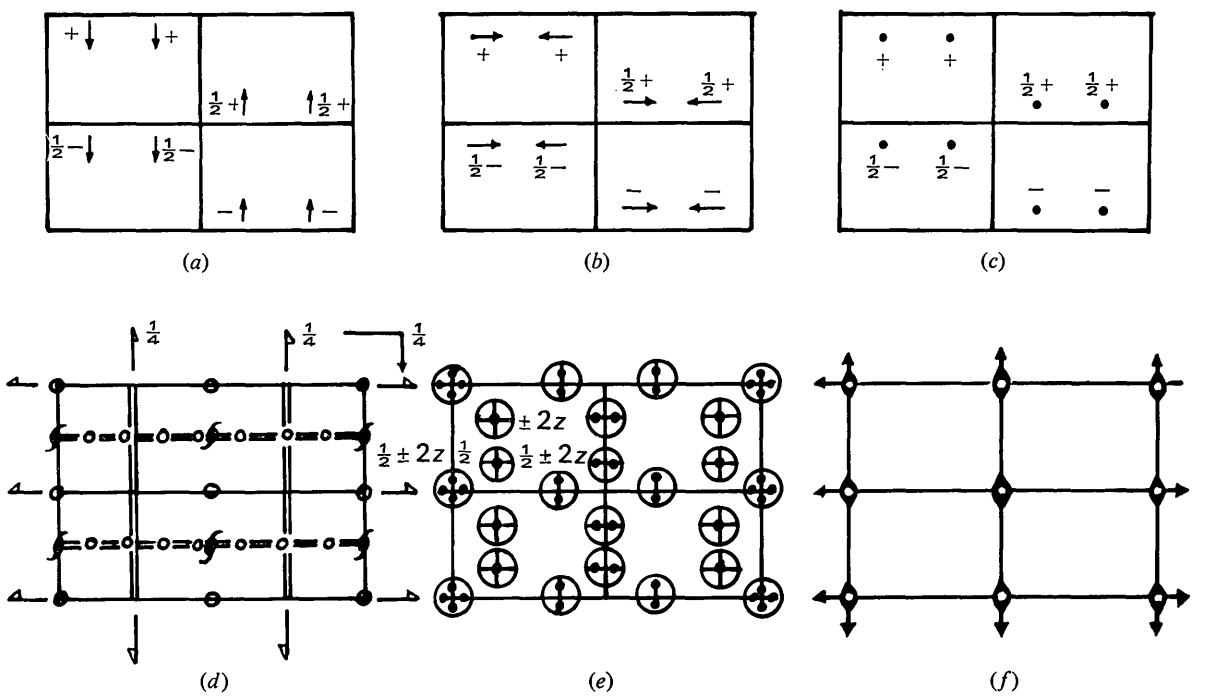

Fig. 5. Effect of space group *Pn'm'a* on (*a*) *x*, (*b*) *y* and (*c*) *z* spin components of atoms in general equivalent position 8(*d*). (*d*) shows the magnetic-space-group symmetry operators while (*e*) contains stereograms drawn at positions of Patterson peaks (with poles indicating the elongation directions) which overlap at that point. (*f*) is the symmetry of (*e*).

single domain when two spins are at right angles [Fig. 1(*c*), structure *B*].

A second feature which can indicate domain overlap is a precise integral relationship between the magnitudes of peaks in the distribution when this is not demanded by the existing symmetry elements. An example of this is found in the magnetic structures of Mn_2P (Yessik, 1968) and Mn_5Si_3 (Lander, Brown & Forsyth, 1967), where the Patterson distributions produced by Fourier transformation of the observed intensity data are clearly hexagonal with the chemical *a* hexagonal axis doubled. The structures are antiferromagnetic as there are equal amounts of positive and negative Patterson density but this is curiously arranged. The origin peak is of magnitude 3 while at positions $(a,0,0)$, $(0,a,0)$ and $(a,a,0)$ there are equal peaks each of magnitude precisely -1. On detailed examination it becomes clear that the magnetic domains are in fact orthorhombic and that this relationship has arisen because of the overlap of two peaks of magnitude -1 with one of $+1$. This type of effect does not conclusively indicate domain overlap, however, as it can occur in a single domain [Fig. 1(*c*), structure *C*].

In addition to its predictive value for a particular magnetic structure model the Patterson function is more widely useful as it allows a discussion of the information available in neutron-diffraction experiments in general. In this paper, for example, it has been used to extend the conclusions of Shirane on the information available from powder diffraction data.

APPENDIX 1

The expression for the Patterson peak computed from three dimensional data is

$$Q'(\mathbf{u}^{mn}+\mathbf{x})=f_1(|\mathbf{x}|)\mathbf{S}^m\,.\,\mathbf{S}^n+f_2(|\mathbf{x}|)\,(\mathbf{S}^m\,.\,\hat{\mathbf{x}})\,(\mathbf{S}^n\,.\,\hat{\mathbf{x}})$$

and the information on the elongation of this peak relative to the reference axes is contained in the product $(\mathbf{S}^m\,.\,\hat{\mathbf{x}})\,(\mathbf{S}^n\,.\,\hat{\mathbf{x}})$. Consider a material with tetragonal configurational symmetry. There will be in the simplest case four domain types for this material and when thePatterson distributions for these domains are superposed there will be at the position $\mathbf{u}_{mn}$ four overlapped peaks which arise from pairs of spins with components

$$\begin{array}{llll} S_1^m, & S_2^m, & S_3^m & -S_1^m, -S_2^m, \quad S_3^m \\ S_1^n, & S_2^n, & S_3^n & -S_1^n, -S_2^n, \quad S_3^n \\ S_2^m, & -S_1^m, & S_3^m & -S_2^m, \quad S_1^m, \quad S_3^m \\ S_2^n, & -S_1^n, & S_3^n & -S_2^n, \quad S_1^n, \quad S_3^n \end{array}$$

relative to orthogonal reference axes 1, 2 and 3 with the tetrad parallel to axis 3.

The average of these four peaks is therefore

$$\overline{Q'(\mathbf{u}^{mn}+\mathbf{x})}=f_1(|\mathbf{x}|)\mathbf{S}^m\,.\,\mathbf{S}^n+f_2(\mathbf{x}|)\,(\mathbf{S}^m\,.\,\hat{\mathbf{x}})\,(\mathbf{S}^n\,.\,\hat{\mathbf{x}})$$

and

$$\begin{aligned}&\overline{(\mathbf{S}^m\,.\,\hat{\mathbf{x}})\,(\mathbf{S}^n\,.\,\hat{\mathbf{x}})}\\ &=\tfrac{1}{4}\{(S_1^mx_1+S_2^mx_2+S_3^mx_2)\,(S_1^nx_1+S_2^nx_2+S_3^nx_3)\\ &+(S_2^mx_1-S_1^mx_2+S_3^mx_3)\,(S_2^nx_1-S_1^nx_2+S_3^nx_3)\\ &+(-S_1^mx_1-S_2^mx_2+S_3^mx_3)\,(-S_1^nx_1-S_2^nx_2+S_3^nx_3)\\ &+(-S_2^mx_1+S_1^mx_2+S_3^mx_3)\,(-S_2^nx_1+S_1^nx_2+S_3^nx_3)\}\\ &=\tfrac{1}{2}(S_1^mS_1^n+S_2^mS_2^n)\,(x_1^2+x_2^2)+S_3^mS_3^nx_3^2\\ &=\tfrac{1}{2}(S_1^mS_1^n+S_2^mS_2^n)\,(1-x_3^2)+S_3^mS_3^nx_3^2\,.\end{aligned}$$

$\therefore$

$$\begin{aligned}\overline{Q'(\mathbf{u}^{mn}+\mathbf{x})}&=f_1(|\mathbf{x}|)\mathbf{S}^m\,.\,\mathbf{S}^n\\ &+f_2(|\mathbf{x}|)\{\tfrac{1}{2}(\mathbf{S}_1^mS_1^n+S_2^mS_2^n)\,(1-x_3^2)+S_3^mS_3^nx_3^2\}\end{aligned}$$

which depends not on x_1 and x_2 but only x_3. It is therefore not possible to determine the angle which the spins $\mathbf{S}^m$, $\mathbf{S}^n$ make with the x_1 and x_2 axes.

Similar analyses may be made of the other systems with the following results.

Trigonal and hexagonal configurational symmetries

Average taken over three domains with triad or hexad parallel to x_3 axis. Pairs of spin components are

$$\begin{array}{ll} S_1^m,\ S_2^m,\ S_3^m & \tfrac{1}{2}(-S_1^m+\sqrt{3}S_2^m),\quad -\tfrac{1}{2}(\sqrt{3}S_1^m+S_2^m),\ S_3^m \\ S_1^n,\ S_2^n,\ S_3^n & \tfrac{1}{2}(-S_1^n+\sqrt{3}S_2^n),\quad -\tfrac{1}{2}(\sqrt{3}S_1^n+S_2^n),\ S_3^n \\ & -\tfrac{1}{2}(S_1^m+\sqrt{3}S_2^m),\ \tfrac{1}{2}(\sqrt{3}S_1^m-S_2^m),\ S_3^m \\ & -\tfrac{1}{2}(S_1^n+\sqrt{3}S_2^n),\ \tfrac{1}{2}(\sqrt{3}S_1^n-S_2^n),\ S_3^n \end{array}$$

$$\begin{aligned}\overline{Q'(\mathbf{u}^{mn}+\mathbf{x})}&=f_1(|\mathbf{x}|)\mathbf{S}^m\,.\,\mathbf{S}^n\\ &+f_2(|\mathbf{x}|)\{\tfrac{1}{2}(S_1^mS_1^n+\,+S_2^mS_2^n)\,(1-x_3^2)+S_3^mS_3^nx_3^2\}\,.\end{aligned}$$

Orthorhombic configurational symmetry

Average taken over four domains with spin components

$$\begin{array}{llll} S_1^m, & S_2^m, & S_3^m & S_1^m, \ -S_2^m, \ S_3^m \\ S_1^n, & S_2^n, & S_3^n & S_1^n, \ -S_2^n, \ S_3^n \\ -S_1^m, & -S_2^m, & S_3^m & -S_1^m, \quad S_2^m, \ S_3^m \\ -S_1^n, & -S_2^n, & S_3^n & -S_1^n, \quad S_2^n, \ S_3^n \end{array}$$

$$\begin{aligned}Q'(\mathbf{u}^{mn}+\mathbf{x})&=f_1(|\mathbf{x}|)\mathbf{S}^m\,.\,\mathbf{S}^n\\ &+f_2(|\mathbf{x}|)\{S_1^mS_1^nx_1^2+S_2^mS_2^nx_2^2+S_3^mS_3^nx_3^2\}\,.\end{aligned}$$

Monoclinic configurational symmetry

Average taken over two domains with spin components

$$\begin{array}{llll} S_1^m, & S_2^m, & S_3^m & -S_1^m, \ S_2^m, \ -S_3^m \\ S_1^n, & S_2^n, & S_3^n & -S_1^n, \ S_2^n, \ -S_3^n \end{array}$$

and diad axis parallel to axis 2.

$$\begin{aligned}\overline{Q'(\mathbf{u}^{mn}+\mathbf{x})}&=f_1(|\mathbf{x}|)\mathbf{S}^m\,.\,\mathbf{S}^n+f_2(|\mathbf{x}|)\{S_1^mS_1^nx_1^2\\ &+S_2^mS_2^nx_2^2+S_3^mS_3^nx_3^2+(S_2^mS_1^n+S_3^mS_3^n)x_1x_3\}\,.\end{aligned}$$

Cubic configurational symmetry

Average taken over twelve domains by consideration of four trigonal axes (each with three domains) in cubic ⟨111⟩ directions.

$$\overline{Q'(\mathbf{u}^{mn}+\mathbf{x})}=S^m \cdot S^n\{f_1(|\mathbf{x}|)+\tfrac{1}{3}f_2(|\mathbf{x}|)\} .$$

References

ATOJI, M. (1965). *Amer. J. Phys.* **33**, 212–219.
AUSTIN, A. E., ADELSON, E. & CLOUD, W. H. (1963). *Phys. Rev.* **131**, 1511–1517.
BUERGER, M. J. (1950). *Acta Cryst.* **3**, 87–97.
FORSYTH, J. B., JOHNSON, C. E. & WILKINSON, C. (1970). *J. Phys. C*, **3**, 1127–1139.
KOEHLER, W. C., WOLLAN, E. O. & WILKINSON, M. K. (1960). *Phys. Rev.* **118**, 58–70.
LANDER, G. H., BROWN, P. J. & FORSYTH, J. B. (1967). *Proc. Phys. Soc.* **91**, 332–340.
LI, Y. Y. (1955). *Phys. Rev.* **100**, 627–631.
OPECHOWSKI, W. & GUCCIONE, R. (1965). *Magnetism*, Vol. IIA. Chap. 3, Edited by G. T. RADO and H. SUHL. New York: Academic Press.
ROTH, W. L. (1960). *J. Appl. Phys.* **31**, 2000–2011.
SHIRANE, G. (1959). *Acta Cryst.* **12**, 282–285.
SHULL, C. G., STRAUSER, W. A. & WOLLAN, E. O. (1951). *Phys. Rev.* **83**, 333–345.
WILKINSON, C. (1968). *Phil. Mag.* **17**, 609–621.
WILKINSON, C. (1973). *Acta Cryst.* A**29**, 449–452.
YESSIK, M. (1968). *Phil. Mag.* **17**, 623–632.

Acta Cryst. (1973). A**29**, 461

Prediction of Partially Recorded Reflexions on Screenless Precession Photographs

BY M. LEIJONMARCK, O. RØNNQUIST AND P.-E. WERNER

Institute of Inorganic and Physical Chemistry, University of Stockholm, S-104 05 Stockholm, Sweden

(*Received* 28 *November* 1972; *accepted* 6 *February* 1973)

Three-dimensionally valid equations for the prediction of partially recorded reflexions on screenless precession photographs are proposed. The equations are based on a discussion of the mosaic spread of the crystal. Applications to the collection of 5 Å resolution data from hexon, a surface protein in the shell of adenovirus [Franklin, R. M., Harrison, S. C., Pettersson, U., Philipson, L., Brändén, C. J. & Werner, P.-E. (1971). *Cold Spring Harbor Symposia on Quantitative Biology*. Vol. XXXVI, pp. 503–510] are given.

Introduction

The theory of screenless precession photography has recently been given by Xuong & Freer (1971). The present paper deals with the problem of partially recorded reflexions on screenless precession photographs.

The screenless precession method provides an increased efficiency of data collection over normal layer-line precession photography. The exposure time is decreased by an order of magnitude because of the smaller precession angle required. A reduced exposure time is particularly important for crystals with large unit cells and crystals that suffer radiation damage. We have therefore adopted the screenless precession method for data collection from hexon from adenovirus type 2. The unit cell under investigation is cubic with a cell edge of 149·9 Å.

Fig. 1 is a section through the reciprocal lattice that shows, within the shaded area, the region recorded on a screenless precession photograph. The ξ_{min} and ξ_{max} must be calculated for each ζ in order to determine the recordable portion of the corresponding reciprocal-lattice plane. It was pointed out by Xuong & Freer (1971) that a complete reflexion cannot be recorded for reciprocal lattice points that lie too near the cut-off limits ξ_{min} and ξ_{max}. They also suggest that the partially recorded reflexions are those for which c, as given by

$$c=f\lambda|\xi_{max}-\xi| \quad (1)$$

or

$$c=f\lambda|\xi_{min}-\xi| , \quad (2)$$

is smaller than the film spot size for this reflexion. In equations (1) and (2) f denotes the crystal-to-film distance and λ the wavelength of the radiation used. It is obvious from Fig. 1 however, that the detection of partially recorded reflexions is a three-dimensional problem. Thus the **z** direction must also be taken into account. When the data collection from hexon started we were not aware of this fact. However, the problem was discussed with colleagues, at the Protein Crystallography Workshop in Alpbach in 1972, and an extension of the equations (1) and (2) to the ζ direction led to the erroneous conclusion (see below) that for precession angles around 1° almost all reflexions with d spacings above 10 Å would be partially recorded.